Computed vibrational excitation of CF_4 by low-energy electrons and positrons: Comparing calculations and experiments

J. Franz,[1] I. Baccarelli,[2] S. Caprasecca,[3] and F. A. Gianturco[4,*]

[1]*Department of Physics and Astronomy, University College London, Gower St., London WC1E6BT, United Kingdom*

[2]*Supercomputing Consortium for University and Research, CASPUR, via dei Tizii 6, 00185 Rome, Italy*

[3]*Department of Physics and Astronomy, The Open University, Walton Hall, Milton Keynes MKT76AA, United Kingdom*

[4]*Department of Chemistry, University of Rome La Sapienza, Piazzale A. Moro 5, 00185 Rome, Italy*

(Received 4 December 2008; published 22 July 2009)

Quantum calculations for the excitation of the asymmetric modes of the CF_4 target gas, ν_3 and ν_4, by impact of low-energy electrons and positrons are carried out in the energy range around 1 eV and are compared with recent experimental findings. The similarities and differences between the two types of projectiles, and the two different modes, are analyzed and discussed *vis à vis* the present accord with the experimental results.

DOI: 10.1103/PhysRevA.80.012709 PACS number(s): 34.80.Uv, 34.80.Bm, 34.50.−s

I. INTRODUCTION

The increasing presence of a variety of high-quality measurements, which involve positrons or electrons as low-energy, high-resolution probes of molecular processes in gases and surfaces [1–4] has made even more necessary the setting up of computational and theoretical treatments for such processes, at the nanoscopic level, which would allow us to gain an increasingly clearer, and reliable, understanding of the forces at play and of the mechanisms, which drive their evolution. The possibility of comparing the relative strength and energy behavior of the same elementary processes, for the same molecular targets, when they are generated by either electron or positron beams under very similar conditions is, in fact, very useful for unraveling the changes in the interplay of the forces describing the interaction of the two different probes and for establishing the relative importance, at the fundamental level, of the dynamical differences induced by changing the sign of the impinging elementary charge.

This type of comparison becomes particularly intriguing when it involves energy transfer processes between the low-energy beams of electrons or positrons and the internal degrees of freedom of the target gas (e.g., rotations and/or vibrations), since for such situations one needs to achieve an experimental quality, which permits the direct observation of individual final channels of energy distribution among different rovibrational levels in the gas. As a theoretical and computational challenge, one further needs to be able to describe realistically the quantum-dynamical coupling between the impinging charge and the molecular motions during the low-energy interaction (e.g., see Ref. [5,6]).

Unfortunately, not many examples exist of such detailed comparisons since one has to face the double difficulty of, on one hand, achieving a very high level of energy resolution with both electrons and positrons that allows for the reliable observation, at the same quality level, of individual excitation and de-excitation processes in a polyatomic gas and, on the other hand, of being able to obtain realistic descriptions of the collisional dynamics, at the quantum molecular level, for the state-to-state energy transfer processes involving both types of projectiles.

The present study therefore constitutes an explicit attempt at carrying out this very type of comparison for one of the most popular polyatomic gases, the carbon tetrafluoride (CF_4), that is made to interact with both positrons and electrons in the low-energy regimes. We have actually analyzed in the past the outcomes of calculations involving the scattering of electrons [7,8] and positrons [9,10] with gaseous CF_4. However, none of the previous studies looked at vibrational excitation processes using an "exact" vibrational coupled-channel expansion nor we have explicitly compared results for both leptonic particles on the title molecule as we do in the present work. The main thrust of this work will therefore be a theoretical and computational analysis of two of the normal modes describing the internal motion of the target molecule when excited by electron or positron impact at low energies.

The work is organized as follows: the next Sec. II outlines the theoretical treatments which we employ to describe electron- and positron-impact vibrational excitations of gaseous CF_4, while Sec. III reports the results of our calculations for both elementary projectiles and compares them with available experiments for the same processes. Sec. IV finally summarizes our conclusions.

II. COMPUTATIONAL TOOLS

A. Scattering Equations

The details of the present theory have been already reported in our previous work [5,6], so we provide here to the reader only a brief reminder of it. In order to obtain vibrational excitation cross sections for positron and electron scattering from polyatomic molecules we need to solve the Schrödinger equation of the total system to yield the total wave function Ψ at a fixed value of the total energy E. It should also be noted that no positronium (Ps) formation channel is considered throughout the present calculations as this process is estimated to be fairly negligible at the energies we are considering. Furthermore, in the case of the e^- pro-

*Corresponding author; fagiant@caspur.it

jectile we shall only consider vibrational excitation of the CF_4 gas as being the chief energy-transfer process at these energies.

We also assume that the orientation of the target molecule is being kept fixed during the collision since molecular rotations are usually slower when compared with the velocity of the projectile. This is called the fixed-nuclear orientation (FNO) approximation [4], and corresponds to ignoring the rotational Hamiltonian of the total system. Then, the total wave function could be generally expanded as follows:

$$\Psi(\mathbf{r}_\mathrm{p}|\mathbf{R}) = r_\mathrm{p}^{-1}\sum_{l\nu n} u_{l\nu n}(r_\mathrm{p})X_{l\nu}(\hat{\mathbf{r}}_\mathrm{p})\chi_n(\mathbf{R}). \tag{1}$$

Here, χ_n is the vibrational wave function of the molecule with the vibrational quantum number $n \equiv (n_1, \ldots, n_N)$ with N representing the total number of normal vibrational modes of the target molecule. The variables $\mathbf{R}$ and $\mathbf{r}_\mathrm{p}$ now denote the molecular nuclear geometry and the position vector of the scattered projectile from the center-of-mass (c.m.) of the target, respectively. The unknown functions $u_{l\nu n}$ describe the radial coefficients of the wave function of the incident particle and the $X_{l\nu}$ are the symmetry-adapted angular basis functions [11]. In this paper, ν in Eq. (1) stands for the indices $(p\mu h)$ collectively, where p stands for the chosen irreducible representation, μ distinguishes the component of the basis if its dimension is greater than one, and h does that within the same set of (pl).

After substituting Eq. (1) into the equation of the total collision system under the FNO approximation, we obtain for $u_{l\nu n}(r_\mathrm{p})$ a set of full coupled-channel equations which now also include vibrational channels. These are called the body-fixed vibrational coupled-channel (BF-VCC) equations ([4,5,12])

$$\left\{\frac{d^2}{dr_\mathrm{p}^2} - \frac{l(l+1)}{r_\mathrm{p}^2} + k_n^2\right\}u_{l\nu n}(r_\mathrm{p}) = 2\sum_{l'\nu' n'} \langle l\nu n|V|l'\nu' n'\rangle u_{l'\nu' n'}(r_\mathrm{p}), \tag{2}$$

where $k_n^2 = 2(E - E_n^{vib})$ with E_n^{vib} being the energy of the specific molecular vibration we are considering. Any of the elements of the interaction matrix in Eq. (2) is given by

$$\langle l\nu n|V|l'\nu' n'\rangle = \sum_{l_0\nu_0}\int d\mathbf{R}\{\chi_n(\mathbf{R})\}^* V_{l_0\nu_0}(r_\mathrm{p}|\mathbf{R}) \times\{\chi_{n'}(\mathbf{R})\}\int d\hat{\mathbf{r}}_\mathrm{p} X_{l\nu}(\hat{\mathbf{r}}_\mathrm{p})^* X_{l_0\nu_0}(\hat{\mathbf{r}}_\mathrm{p})X_{l'\nu'}(\hat{\mathbf{r}}_\mathrm{p}). \tag{3}$$

This method is essentially a generalization of the method proposed long ago (called the "hybrid theory") for the simple case of a diatomic molecule [13]. When solving Eq. (2) under the boundary conditions that the asymptotic form of $u_{l'\nu' n'}^{l\nu n}$ is represented by a sum containing the incident plane wave of the projectile and the outgoing spherical wave, we obtain the necessary K-matrix elements from which the relevant T-matrix is constructed. Therefore, the integral cross section for the vibrationally inelastic scattering is given by

$$Q(n \to n') = \frac{\pi}{k_n^2}\sum_{l\nu}\sum_{l'\nu'}|T_{l'\nu' n'}^{l\nu n}|^2, \tag{4}$$

where $T_{l'\nu' n'}^{l\nu n}$ is the T-matrix element for that process [12].

In the case of positrons as projectiles, the interaction potential (V) between the latter elementary charge and the molecular target is represented in the form of a local potential. Thus, V is described by the sum of the repulsive electrostatic (V_{st}) and the attractive positron correlation-polarization (V_{pcp}) terms. For the latter term we have employed over the years [14] the simple, parameter-free model potential introduced by Boronski and Nieminen [15] for the short-range region of r_p, and have connected it smoothly with the asymptotic form of the polarization potential $-\alpha_0/2\mathbf{r}_\mathrm{p}^4$, with α_0 being the spherical dipole polarizability of the target.

A simpler computational method which has often been employed to treat vibrational excitation is called the adiabatic nuclear vibration (ANV) approximation (see, e.g., [16]) where no direct vibrational dynamical coupling [like it occurs in Eq. (3)] is active during the scattering process [17]. However, we shall not be using this method in the present work since we already generate the correct coupling matrix elements of Eq. (3) and we have already compared the ANV results with correct coupled-channel (CC) results in previous work of our group (e.g., see Refs. [16,17]), where we found our results to be very similar at energies away from threshold. Since we already use here the "exact" CC results no such comparison with a more approximate method will be presented in this paper.

In the case of the scattering of electron beams from the target molecule, the fermionic nature of the $(N+1)$ interacting electrons requires the inclusion of an additional force which originates from the exchanging effects between bound and continuum electrons [12]. In the present treatment we have resorted to a model exchange interaction which we have used many times before and which has been reported in detail in our earlier work [18,19]. Suffice it to say here that the chief simplification of this modeling is to disregard the local momentum of the bound electrons with respect to that of the impinging projectile, thereby neglecting the gradients of the occupied molecular orbitals with respect to that of the continuum wave function for the scattered electron.

For the electron-molecule long-range polarization terms and the short-range dynamical correlation effects we have implemented a local, energy-independent model potential, $V_{\mathrm{ecp}}(\mathbf{r})$ already discussed previously in our work [20,21]. Briefly, the $V_{\mathrm{ecp}}(\mathbf{r})$ potential contains a short-range correlation contribution, V_{corr}, which is smoothly connected to a long-range polarization contribution, V_{pol}, both terms being specific for electron projectiles. The short-range term is obtained by defining an average dynamical correlation energy of a single electron within the formalism of the Kohn and Sham variational orbitals representing the bound electrons [20]. The functional derivative of such a quantity with respect to the selfconsistent field (SCF) N-electron density of the molecular target provides a density-functional description of the required short-range correlation term (for a general discussion of density functional theory methods see [22]).

The long-range part of V_{ecp} is obtained by first constructing a model polarization potential, V_{pol}, which asymptotically agrees with the potential obtained from the static dipole polarizability of the target in its ground electronic state: this corresponds to including the dipole term in the second-order perturbation expansion of the polarization potential. Since in the general case the long-range contribution, V_{pol}, does not exactly match the short-range correlation, V_{corr}, at any given value of r, one needs an appropriate r_{match} by first performing a single-center expansion of both contributions and by then finding where the two radial coefficients for $l=0$ first intersect. This has, in fact, been what we found in many cases to be the more effective choice in terms of the global smoothness of the total potential. The matching functions are chosen such that each term added to V_{pol} at distances larger than r_{match} has the same functional form as the first term neglected in the perturbation expansion of V_{pol}. The full interaction corresponds to performing our scattering calculations using the static-exchange correlation-polarization (SECP) interaction. We shall see in the following comparison of our results with experimental findings that the global V_{SECP} interaction, besides being capable of providing a very realistic description of, and nearly quantitative agreement with, the experimental values of the elastic (rotationally summed) integral cross sections at low energies for CF_4 [23,24], also performs very well for the description of the vibrationally inelastic low-energy cross sections discussed here.

B. Computational Details

The above model potentials, assembled for both electrons and positrons as impinging projectiles, were first employed to generate the elastic scattering cross sections for the target molecule kept at a fixed geometry, although we shall not repeat here the analysis of those data [10,23,24].

The CF_4 was kept at its equilibrium geometry ($R_{C\text{-}F}=1.320$ Å) and in its ground electronic state. Using the Gaussian suite of codes [25] with 80 basis functions (D95* basis set), the total electronic energy was found to be −435.7654 Hartrees. The experimental dipole polarizability of $\alpha_0=19.6\ a_0^3$ was used within the V_{pol} interaction [26]. This was done to test agreement with our earlier work [23], which was then found to be excellent. The vibrational cross sections additionally required the extention of all the terms of the model potential described before as functions of the nuclear geometries that contribute to the two normal modes. Thus, the changes in the bound-electron density as a function of the dimensionless normal coordinates Qs [27] provided the link with the ensuing changes in the static, exchange, and correlation contributions. We further computed the dipole polarizabilities as a function of normal coordinates and scaled their values at R_{eq} to the experimentally known polarizability mentioned above. The final potential in Eq. (2) was therefore obtained as a function of the relevant molecular geometries. Representative behaviors of such potentials for T_d-symmetry vibrations were reported in our earlier work on tetrahedral molecules [16].

The bottleneck of the method is the evaluation of the potential coupling matrix, an operation which scales very unfavorably with increasing l_{max}. Furthermore, the exchange potential being energy dependent, the coupling matrix must be computed for each energy value. Our present calculations are therefore limited to $l_{max}=80$ in the expansion of the scattering wave function, requiring $\lambda_{max}=160$ in the expansion of the interaction potential. We shall see below that all the cross sections of interest reached convergence within a smaller range of terms in the partial wave expansion and therefore that the above expansion parameters are sufficiently large to yield reliable computed cross sections.

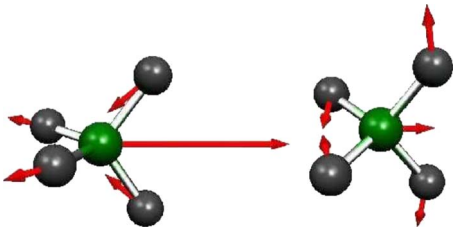

FIG. 1. (Color online) Pictorial representation of the two antisymmetric vibrational modes of CF_4 which we are considering in the present work: on the left we show the stretching mode ν_3 while on the right we represent the bending mode ν_4.

In order to achieve a higher accuracy for the integration over the vibrational motions in the integrals of Eq. (3), and a better description of the vibrational wave functions involved in the coupling terms, we used the quantum chemistry code TURBOMOLE [28] instead of the previously used one [25], so that we had a better control of the chosen Abelian subgroups and a higher accuracy on the set of normal coordinate values employed to generate the integration grid in Eq. (3). We report in Fig. 1 the pictorial view of the two normal modes considered in the present work: on the left we show the antisymmetric stretching mode (ν_3), which is one of the three degenerate components of that infrared active vibrational motion. On the right we report instead the pictorial representation of the antisymmetric bending mode (ν_4), of which we also show one of the three degenerate components.

Our calculated vibrational frequency for the ν_3 mode was 1461.63 cm^{-1}, to be compared with the experimental value (e.g., see Ref. [29]) of 1281 cm^{-1}. With the same token, the computed value for the ν_4 transition is 690.64 cm^{-1} versus the experimental value of 636 cm^{-1} [29]. It is interesting to note from the figure that in the stretching mode the central carbon atom is clearly undergoing large-amplitude motion in comparison with the four fluorine atoms, while in the bending mode all five atoms undergo similar amplitude motions.

Since both the above modes are infrared active, it means that during the vibrational excitation process a permanent dipole moment is induced in the molecule because of its distortion from the equilibrium Td geometry. The behavior of the dipole moments for both normal modes (shown by the plots of Fig. 2), was calculated over the grid of **R** values chosen to describe the two asymmetric deformations reported by Fig. 1. The actual values of the Qs were obtained as the usual linear combinations of bond distances and angles, as given in [7–10].

We evaluated the above quantity over a range of 15 nuclear geometries ranging from $Q=-6.0$ to $Q=+6.0$. The

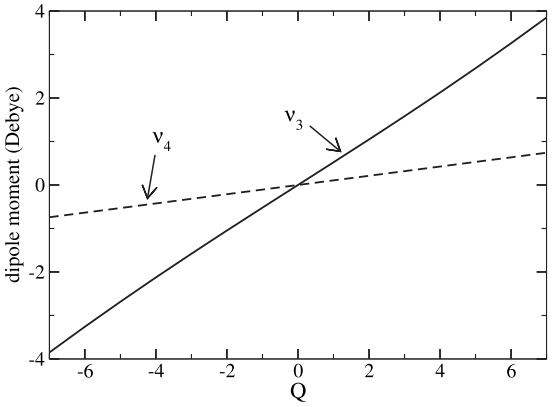

FIG. 2. Computed permanent dipole moments for the two vibrational modes discussed in this work, as functions of the different nuclear geometries associated with the shown range of Q values.

transition moments are thus obtained from the data of Fig. 2 by using the relation

$$M_{if}^{n=\nu_3,\nu_4} = 3\left[\frac{d\mu(Q)}{dQ}\right], \tag{5}$$

where 3 is the degeneracy for both modes. The experimental values [30] are 0.045 a.u. for the ν_3 mode and 0.0012 a.u. for the ν_4. Our calculated values keep the same trend: the $M_{if}^{\nu_3}$ is, in fact, 0.0501 a.u., slightly larger than experiments, while the $M_{if}^{\nu_4}$ is even larger than experiments: 0.0069 a.u. However, one clearly sees from the behavior of the two computed dipoles in Fig. 2 that the variations of μ_3 for the stretching motion are much larger than those exhibited by μ_4, the dipole moment associated with the asymmetric bending, a result which bears clear consequences, as we shall discuss below, on the relative efficiency of the excitation processes for both electrons and positrons.

Similarly, for each relevant nuclear arrangement we calculated the corresponding values of the spherical dipole polarizabilities, which were then uniformly shifted so that the value at the equilibrium geometry matched the experimental value of $19.6a_0^3$ [31]. The shifted values are reported in Fig. 3 as a function of Q for the two normal modes. The computed data, albeit to be taken as a simple modeling of the Q dependence of α_0, clearly show that the ν_3 mode causes much larger changes of that observable with respect to those for the ν_4 excitation, a feature which is indeed related to the differences we shall find in the corresponding excitation cross sections that we discuss in the next section.

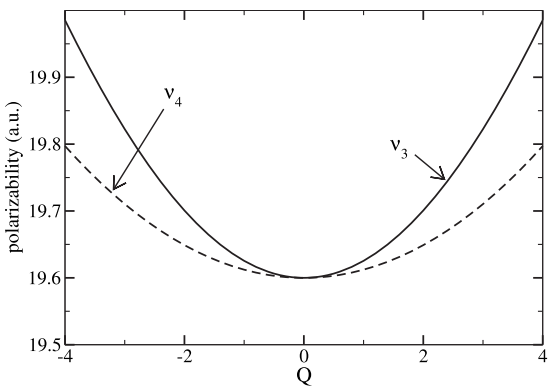

FIG. 3. Shifted values of the computed spherical polarizabilites for the two vibrational modes discussed in this work.

The previously mentioned excitation energies for the $(0 \rightarrow 1)$ transitions are 159 meV for the ν_3 mode and 78 meV for the ν_4 mode: the larger energy gap involved for the asymmetric stretching motion partly explains its higher likelihood for experimental observation [32–35] as opposed to the ν_3 mode which would cause an energy loss effect that would be much harder to detect [32]. Furthermore, our findings on the behavior of the associated M_{if}^{n} values confirm the higher visibility of the ν_4 excitation found by the experiments described below. Finally, our convergence tests on the number of vibrational channels, which we include in Eq. (2) showed that, for electron collisions, one needed to include at least two closed channels in the expansion while, for positron scattering, no closed channels were needed. Both results indeed confirm our earlier findings on polyatomic systems [36,37].

III. COMPARISON WITH EXPERIMENTS

A. Vibrational Excitation Processes

As mentioned in the Introduction, the gaseous CF_4 is considered to be an important species to be studied in positron impact experiments because of its relevance on being used as a rapid cooling interface in buffer-gas positron accumulators [38] and also for cooling positron plasmas in Penning-Malmberg traps [39]. It therefore becomes important to be able to estimate its capability of efficiently undergoing transfers of collision energy to its network of vibrational modes, the ν_3 one being the most likely candidate for such energy-transfer process [33]. In the case of electron-impact inelastic processes with CF_4, it is just as important to be able to assess the size and energy behavior of its excitation cross sections since excited carbon tetrafluoride is known to undergo several possible fragmentation reactions when it is made to interact with low-energy electron beams, reactions which strongly depend on its level of internal excitation [40].

It therefore follows that to obtain specific experimental and computational data which can help us to compare the behavior of different vibrational modes, and for different types of elementary projectiles (e.g., electrons and positrons in the low-energy regimes) is of great interest and has been pursued by several earlier studies (e.g., see Refs. [41,42]). One of the most recent works has directly compared the ν_3 behavior, for both e^+ and e^- as projectiles [32], in experiments at the low-energy regime: we shall therefore seek to analyze their experimental findings *vis á vis* our present calculations for the same excitation process.

An interesting result from our calculations is reported by the data in Fig. 4, where the excitation processes for ν_3 and ν_4 are presented to test the convergence of our partialwave expansion, and where we also compare our findings for both electrons and positrons as probes of the vibrational-excitation process.

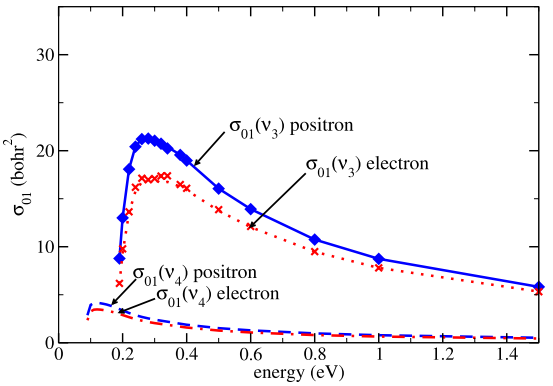

FIG. 4. (Color online) Computed inelastic cross sections for electron and positron impact excitation of CF_4 vibrational modes, ν_3 and ν_4, discussed in the main text. No correlation-polarization forces have been included in the above computations. See main text for details.

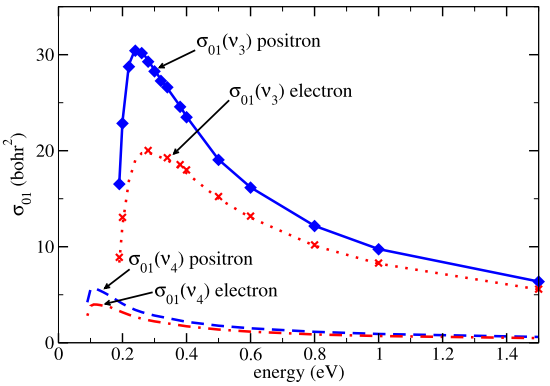

FIG. 5. (Color online) Computed $(0\rightarrow 1)$ excitation cross sections for the two asymmetric modes (ν_3 and ν_4) and for both types of projectiles. See main text for details.

Several comments can be made from a perusal of the calculations presented in that figure:

• the numerical convergence of the inelastic cross sections obtained by e^+ impact is rather good, we see that the solid line and the filled-in lozenges essentially yield the same cross sections, although they correspond to maximum partialwave values of 18 for the lozenges and of 24 for the solid line;

• the same occurs for the electron-impact excitation processes, where we see invariance of the computed cross sections when given by either the light crosses ($l_{max}=18$) or the dots ($l_{max}=24$). To simplify the plot, the data for the ν_4 mode only show the converged results at $l_{max}=24$;

• when calculations are carried out at the static potential level for e^+, and with the additional inclusion of exchange only for e^-, we see that both modes indicate strong similarities in shape and size between the inelastic processes induced by the two projectiles: the positron-impact excitation of the ν_3 mode follows closely the e^--impact results but remains larger than the latter at all energies, although it remains so by no more than 20% over the whole range;

• the excitation of the bending mode ν_4, on the other hand, produces for both projectiles much smaller cross sections, they always remain at least one order of magnitude smaller than the ν_3, at all energies above threshold;

• the transition dipole moments therefore play a dominant role in such calculations and clearly show that the asymmetric stretching deformation is a much more efficient process in the low-energy regimes considered here because of the presence of substantial, nonvanishing permanent dipole contributions.

In conclusion, at the purely static (and static+exchange) level of describing the interactions, the calculations of the vibrational excitation from both charged projectiles indicate two chief results: (i) that the differences in the transition dipole moments translate themselves into large differences in size between stretching and bending excitation cross sections and (ii) that e^+ and e^- give rise to collisional excitations that are very similar for both projectiles, at least for the asymmetric modes examined here.

It therefore becomes of interest to see now what is the effect of correlation-polarization forces on the scattering processes once they are explicitly included in the calculations. The results for both e^+ and e^- as projectiles, for the same asymmetric modes, are reported by Fig. 5. We show there that the inclusion of correlation effects, albeit both modeled, within our treatment, as local forces from density functional theory (DFT) methods (see previous Section) plus the addition of long-range polarization terms which are given by the dipole polarizability, have marked effects on the inelastic cross sections: the expansion convergence, however, is achieved at the same parameter values as in the previous calculations.

The cross sections associated with the bending excitation, the ν_4, are seen to change very little upon the inclusion of the V_{cp} potentials; those from the electron-impact collisions are essentially unchanged, while those from positron scattering have increased by about 10% with respect to those of Fig. 4. The asymmetric distortion generated by that mode, as we can see from its pictorial view in Fig. 1, is creating a net correlation effect around the nuclei which essentially cancels over the global excursion of this normal coordinate, as it occurs for long-range polarization changes. This cancellation is more marked for the e^- projectile as it samples more closely the nuclear region with strong, short-range correlation contributions, while less evident for the positron partner which is sampling less closely the short-range region, especially at low collision energies, but is strongly driven by long-range polarization terms.

The situation, however, changes in the case of the asymmetric stretching mode, where the large amplitude motion of the carbon atom now occurs out of phase with respect to the collective motions of the fluorine atoms and therefore strongly modifies the behavior of the dynamical correlation +polarization effects, especially in the case of positron projectiles. We therefore see that the excitation cross section for the ν_3 mode changes more markedly for the case of the e^+ partner, where the V_{cp} contributions now yields an increase in the cross sections around the threshold maximum by more than 40%. On the other hand, the excitation process induced by electrons is modified by correlation effects by a mere 10%, as was the case for the ν_4 excitation.

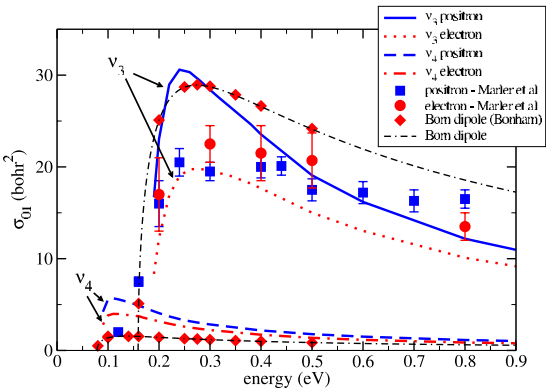

FIG. 6. (Color online) Computed and measured $(0 \rightarrow 1)$ excitation cross sections for the ν_3 asymmetric stretching mode of CF_4 in collision with e^+ and e^-. The experiments (filled squares and filled circles) are from Ref. [32] and the earlier data of Ref. [44] and of Ref. [45] (lozenges) are also reported. Our calculations for the ν_4 mode excitation are also shown, together with our Born-dipole calculations for both modes (dot-dashes).

Since the long-range polarization forces are the same for both projectiles, and since the mode-dependent electrostatic and exchange forces create very similar cross sections for both projectiles (as shown by Fig. 4), we can suggest from our numerical experiment that the short-range correlation changes during the ν_3 excitation are very important since they largely dominate the coupling [43], this being even more so for the positron projectile. We also see from the data in Fig. 5 that such effects are strongly mode-dependent and that stretching motions are more sensitive to the coupling induced by the short-range correlation effects. At the nanoscopic level, we could also note that the stretching deformation of the molecule involves here a larger volume of space than that occupied by it during the more compact asymmetric bending: since our DFT modeling of correlation forces depends on the overall volume occupied by the bound electron probability densities, it then stands to reason that such forces would be more important for the ν_3 excitation than for the ν_4 one. Furthermore, the largely attractive nature of both correlation and polarization effects, and for both e^+ and e^- projectiles, causes the vibrational excitation to increase when the latter potentials are included, as we see in Fig. 5. Finally the absence of exchange forces in the case of e^+ makes that collision partner more effectively coupled to nuclear motions during the ν_3 stretching excitation, hence the inelastic dynamics yields here larger excitation probabilities for the positron case.

As mentioned earlier, recent experimental data have reported excitation of ν_3 and ν_4 modes for CF_4 in collision with both e^+ and e^-, at energies just above the corresponding threshold openings [32]. In that work also earlier estimates of the ν_3 vibrational excitation were reported [44,45], as we shall further discuss below. A comparison of our present results with those data is presented in detail by Fig. 6: no scaling of either computed or measured cross sections has been introduced and all quantities are thus shown on the same absolute scale.

We also report in that figure the cross section estimates obtained by using the simpler Born-dipole approximation [32]. The data for the ν_4 excitation correspond to the calculations given by Ref. [45] (filled lozenges) and those we obtained from the Eq. (2) of Ref. [32]: they are seen to follow closely our computed curves, since all cross section values remain below $5a_0^2$ over the whole range of energies. For the case of the ν_3 excitation we see that the same calculations from Ref. [45] (given by the same symbols as for the ν_4 mode) follow very closely our calculations for the positron projectile, while remaining larger for the electron probe. One may thus argue that the more complex exchange-correlation effects in the latter system are not well modeled by the Born approximation, while this is not the case for positron-impact excitations where no exchange forces exist. The following comments could also be made from an analysis of the data reported in that figure:

(1) the shapes of the computed and experimental cross sections are rather close to each other. The observed maxima for the measurements with both e^+ and e^- appear below 300 meV, which is where the computed inelastic cross sections for both projectiles exhibit their maximum values.

(2) The ν_3 excitation process by electron impact (dotted line) is very close to the measured data, although the computed cross sections beyond their maximum remain about 10% to 20% below experiments. On the whole, however, our calculations confirm the large size of the cross sections found by experiments.

(3) The positron-impact excitation cross sections generated by our calculations turn out to be larger than the experimental data around the region of the maximum while the energy dependence seen by the experiments is well reproduced by our calculations. We also find that in the range between 200 and 400 meV the calculations are larger than measurements while getting closer to the latter below and above those energies.

(4) The earlier estimates of the same excitation cross sections [44,45] employed a Born-dipole approximation which used a scaling of the experimental transition moments. Their size and energy dependence turn out to be in very close agreement with the present calculations.

(5) The calculated excitation cross sections for the asymmetric bending mode ν_4 are seen to be much smaller in size than the experiments for the ν_3 mode, in agreement with the fact that no observation was made for such mode over the same range of energies with both type of projectiles. That mode, therefore, involves an energy-loss probability which is too small to be as yet amenable to detection.

It is also interesting to note the closeness in size shown by the positron calculations and the Born-dipole approximation results obtained with different scaling procedure [44,45] and which are basically independent of the sign of the charge of the projectile. This finding indicates that our model of correlation forces for the case of the positron possibly overestimates their strength and ends up matching the simpler approximation where the dipole-Born cross section is driving the excitation. On the other hand, our correlation modeling for electron-induced vibrationally inelastic collisions turns out to be fairly realistic, yields excitation cross sections in good accord with measurements and performs better than the simplest Born-dipole approximation.

IV. CONCLUSIONS

In the work described in the previous Sections, we have attempted to tackle different aspects of the low-energy scattering features of gaseous CF_4 when made to interact with both positrons and electrons beams:

- to see how well a close-coupling approach to vibrationally inelastic cross sections in a fairly large polyatomic gas can describe existing experiments for positron scattering;
- to verify that the above computational scheme can also be applied with good success to collisions involving beams of low-energy electrons;
- to analyze and explain the differences caused on the same dynamical process (low-energy vibrational excitation by particle impact) when using two different elementary probes as e^+ and e^-.

All the above aspects have been discussed in detail by our calculations and our findings have been shown to agree fairly well with the experimental findings. In particular, we have found that the unusually large inelastic cross sections for the asymmetric stretching mode (ν_3) observed by the experiments [32] are reproduced by the present calculations, both in size and in energy dependence from threshold to about 900 meV, for the two types of charged projectiles, electrons and positrons. We further found that the positron-impact excitation yields larger cross sections than those obtained by electron-impact, provided correlation-polarization forces were included. In particular, we see from the present calculations that purely electrostatic interactions behave similarly for the two projectiles while correlation effects are more significant in the case of positron-impact studies. On the whole, however, the Born-dipole approximation tends to overestimate the experimental inelasticity for both e^- and e^+ projectiles since it does not include the more correct potential effects caused by bound-to-continuum electron density correlation that occurs during vibrations and which is indeed present in our modeling of the interaction.

Our calculations also show why the asymmetric bending (the ν_4 mode) inelastic cross sections have not yet been observed: the corresponding induced dipole is, in fact, smaller than for the case of the ν_3 mode and therefore the size of the corresponding cross sections is below the current detection thresholds of both positron and electron experiments.

The present study constitutes one of the few examples in which experimentally determined vibrational excitations of a polyelectronic, polyatomic molecular target by both electron and positron impact are compared with realistic quantum calculations and analyzed in terms of the interplay between elementary components of the interaction forces which act in both systems.

ACKNOWLEDGMENTS

The financial support of the Committee for Scientific Research of the University of Rome and of the PRIN national Research Network is gratefully acknowledged. The computational support from the CASPUR and CINECA Consortia is also appreciated. One of us (J.F.) also acknowledges the support of the EIPAM ESF Project for a period of stay at the University of Rome while this project was carried out.

[1] C. M. Surko, G. F. Gribakin, and S. J. Buckman, J. Phys. B **38**, R57 (2005).
[2] W. E. Kauppila and T. S. Stein, Adv. At., Mol., Opt. Phys. **26**, 1 (1990).
[3] L. G. Christophorou and J. K. Olthoff, J. Phys. Chem. Ref. Data **28**, 967 (1999).
[4] Y. Itikawa, Int. Rev. Phys. Chem. **16**, 155 (1997).
[5] T. Nishimura and F. A. Gianturco, Nucl. Instrum. Methods Phys. Res. B **221**, 24 (2004).
[6] T. Nishimura and F. A. Gianturco, Phys. Rev. A **65**, 062703 (2002).
[7] M. Cascella, R. Curik, F. A. Gianturco, and N. Sanna, J. Chem. Phys. **114**, 1989 (2001).
[8] S. Irrera and F. A. Gianturco, New J. Phys. **7**, 1 (2005).
[9] F. A. Gianturco, T. Mukherjee, and A. Occhigrossi, Phys. Rev. A **64**, 032715 (2001).
[10] T. Nishimura and F. A. Gianturco, J. Phys. B **37**, 215 (2004).
[11] P. Burke, N. Chandra, and F. A. Gianturco, J. Phys. B **5**, 2212 (1972).
[12] F. A. Gianturco and A. Jain, Phys. Rep. **143**, 347 (1986).
[13] N. Chandra and A. Temkin, Phys. Rev. A **13**, 188 (1976).
[14] *New Directions in Antimatter Chemistry and Physics*, edited by F. A. Gianturco and C. M. Surko (Kluwer, Amsterdam, 2001).
[15] E. Boronski and R. M. Nieminen, Phys. Rev. B **34**, 3820 (1986).
[16] M. Cascella, R. Curik, and F. A. Gianturco, J. Phys. B **34**, 705 (2001).
[17] S. C. Althorpe, F. A. Gianturco, and N. Sanna, J. Phys. B **28**, 4165 (1995).
[18] F. A. Gianturco and S. Scialla, J. Phys. B **20**, 3171 (1987).
[19] F. A. Gianturco, L. C. Pantano, and S. Scialla, Phys. Rev. A **36**, 557 (1987).
[20] F. A. Gianturco, R. R. Lucchese, and N. Sanna, J. Chem. Phys. **100**, 6464 (1994).
[21] F. A. Gianturco, R. R. Lucchese, and N. Sanna, J. Chem. Phys. **104**, 6482 (1996).
[22] R. G. Parr and W. Yang, *Density Functional Theory of Atoms and Molecules* (Oxford University Press, Oxford, 1989).
[23] F. A. Gianturco and K. Willner, Phys. Rev. A **75**, 062714 (2007).
[24] K. Willner and F. A. Gianturco, Phys. Rev. A **74**, 052715 (2006).
[25] M. J. Frisch *et al.*, GAUSSIAN 03, revision c.02, Gaussian, Inc., Wallingford, CT, 2004.
[26] K. J. Miller, J. Am. Chem. Soc. **112**, 8533 (1990).
[27] E. B. Wilson, J. Decius, and P. C. Cross, *The Theory of Infrared and Raman Vibrational Spectra* (Dover, New York, 1980).
[28] R. Ahlrichs, TURBOMOLE version 5, University of Karlsruhe, 2002.

[29] L. M. Sverdlov, M. A. Kouner, and E. P. Krainov, *Vibrational Spectra of Polyatomic Molecules* (Wiley, New York, 1974).
[30] D. M. Bishop and L. M. Cheung, J. Phys. Chem. Ref. Data **11**, 119 (1982).
[31] T. N. Olney, N. M. Cann, G. Cooper, and C. E. Brion, Chem. Phys. **223**, 59 (1997).
[32] J. P. Marler and C. M. Surko, Phys. Rev. A **72**, 062702 (2005).
[33] S. J. Gilbert, R. G. Greaves, and C. M. Surko, Phys. Rev. Lett. **82**, 5032 (1999).
[34] J. P. Sullivan, S. J. Gilbert, J. P. Marler, L. D. Barnes, S. J. Buckman, and C. M. Surko, Nucl. Instrum. Methods Phys. Res. B **192**, 3 (2002).
[35] J. P. Sullivan, S. J. Gilbert, and C. M. Surko, Phys. Rev. Lett. **86**, 1494 (2001).
[36] T. Nishimura and F. A. Gianturco, Europhys. Lett. **65**, 179 (2004).
[37] T. Nishimura and F. A. Gianturco, Eur. Phys. J. D **33**, 221 (2005).
[38] J. P. Sullivan, S. J. Gilbert, J. P. Marler, R. G. Greaves, S. J. Buckman, and C. M. Surko, Phys. Rev. A **66**, 042708 (2002).
[39] R. G. Greaves and C. M. Surko, Phys. Rev. Lett. **85**, 1883 (2000).
[40] L. G. Christophorou, J. K. Olthoff, and M. V. V. S. Rao, J. Phys. Chem. Ref. Data **25**, 1341 (1996).
[41] S. Zhou, H. Li, W. E. Kauppila, C. K. Kwan, and T. S. Stein, Phys. Rev. A **55**, 361 (1997).
[42] M. Kimura, M. Takekawa, Y. Itikawa, H. Takaki, and O. Sueoka, Phys. Rev. Lett. **80**, 3936 (1998).
[43] T. Nishimura and F. A. Gianturco, Phys. Rev. Lett. **90**, 183201 (2003).
[44] A. Mann and F. Linder, J. Phys. B **25**, 545 (1992).
[45] R. A. Bonham, Jpn. J. Appl. Phys., Part 1 **33**, 4157 (1994).